DOI: 10.1002/adma.200502630

Pixellated Photonic Crystal Films by Selective Photopolymerization**

By *Seung-Kon Lee*, *Gi-Ra Yi*,* *Jun Hyuk Moon*, *Seung-Man Yang*,* and *David J. Pine*

Hierarchical microstructures of colloidal crystals have attracted enormous research efforts due to their potential uses in display devices, optical communications, catalytic supports, biosensors, and acoustic materials.[1,2] Recent progress in self-assembly approaches for such microstructures has shown that regular arrays of microspheres can be easily grown by several clever ways based on well-established techniques including coating and epitaxial growth.[3–7] One of the remaining issues in self-assembled colloidal crystals is to create defective or patterned structures for photonic crystals based microdisplay devices, integrated photonic chips, as well as microcavities for extracting or adding light of specific frequencies.[8–10] Over the years, only a few research groups have suggested suitable fabrication methods for the defect engineering of colloidal crystals, including colloidal crystallization inside microchannels, two-photon polymerization, and surface-charge-induced colloidal crystallization.[11–13] However, a practical approach for hierarchical patterns with high resolution at the micrometer scale inside photonic-crystal films is still a challenge. Here, we describe a simple and facile method for 2D arrays of pixellated multicolor mosaic cells by selective photon-induced polymerization in colloidal crystal films.

To tune the reflective colors of colloidal photonic crystals, it is necessary to find a way to control the refractive-index mismatch, lattice constant (or center-to-center distance between particles, or particle sizes), symmetry (or orientation), magnetic permeability, and precisely positioned defects. Among these factors, one of the most simple and feasible to control is the refractive-index contrast between the matrix and the colloidal particles. Previously, Yoshino et al.[14] reported experimental results on heat-induced color tuning of colloidal crystals embedded in a conducting polymer and several other research groups, including Kang et al.,[15] have demonstrated liquid crystal (LC)-based approaches. However, in addition to the manipulation of the refractive index, it is still necessary to be able to pattern colloidal photonic crystals at the micrometer scale for practical applications in photonics devices and microdisplays. To do this, we used the selective reaction of a photocurable prepolymer inside opaline colloidal crystal structures, whereby the refractive indices of the prepolymer and the opaline colloids were perfectly matched in order to avoid scattering-induced blurring of the photoinduced pattern.

As shown in Figure 1, we have explored photolithography for the manipulation of the reflection colors of inverse opals by patterning them. Before any patterning experiments could be carried out on the photonic crystals, high-quality silica opal films needed to be prepared using uniformly sized silica spheres. Here, silica opal films were deposited on glass substrates by a vertical dip-coating method developed by Colvin and co-workers,[16] which is an easy way to fabricate colloidal crystal films with a relatively small number of defects over large areas. To obtain a polymeric inverse opal film as a scaffold structure, a prepolymer of a negative photoresist (SU-8) was infiltrated into the silica opal film and hard-baked under UV exposure (step i). The silica colloids were dissolved with an HF solution leaving behind well-ordered macropores in a face-centered cubic (fcc) lattice (step ii). Then, the silica opal film was peeled off the glass substrate and placed upside down onto a wafer so that the smooth and planar surface was facing outwards. This was an important procedure for the subsequent patterning process. The top of the inverse opal film was covered with a hydrophobic film of polydimethylsiloxane (PDMS) and the same negative photoresist was used to fill the macropores (step iii). Capillary forces drove the photoresist into the macropores, and as the infiltration was completed the film became transparent. At the soft-baking step, the film remained transparent, which implied that the refractive indices of the inverse opal scaffold and injected photoresist (SU-8) were almost the same. In our previous work, we reported that the refractive indices of hard-baked and soft-baked negative photoresists of SU-8 were 1.5929 and 1.5925, respectively.[17] This small difference in refractive index did not cause any scattering of the UV beam, which would be seen in a corona around the patterns. Finally, UV light was

[*] Dr. G.-R. Yi
Advanced Materials R&D, LG Chem Research Park
Daejeon, 305–380 (Korea)
E-mail: yigira@lgchem.com
Prof. S.-M. Yang, S.-K. Lee, Dr. J. H. Moon
Center for Integrated Optofluidic Systems and
Department of Chemical and Biomolecular Engineering
Korea Advanced Institute of Science and Technology
Daejeon 305–701 (Korea)
E-mail: smyang@kaist.ac.kr
Prof. D. J. Pine
Department of Physics, New York University
New York, NY 10003 (USA)

[**] This work was supported by a grant from the Creative Research Initiative Program of the Ministry of Science and Technology for "Complementary Hybridization of Optical and Fluidic Devices for Integrated Optofluidic Systems". We also appreciate the partial financial support from the Brain Korea 21 Program. Supporting Information is available online from Wiley InterScience or from the author.

ADVANCED MATERIALS

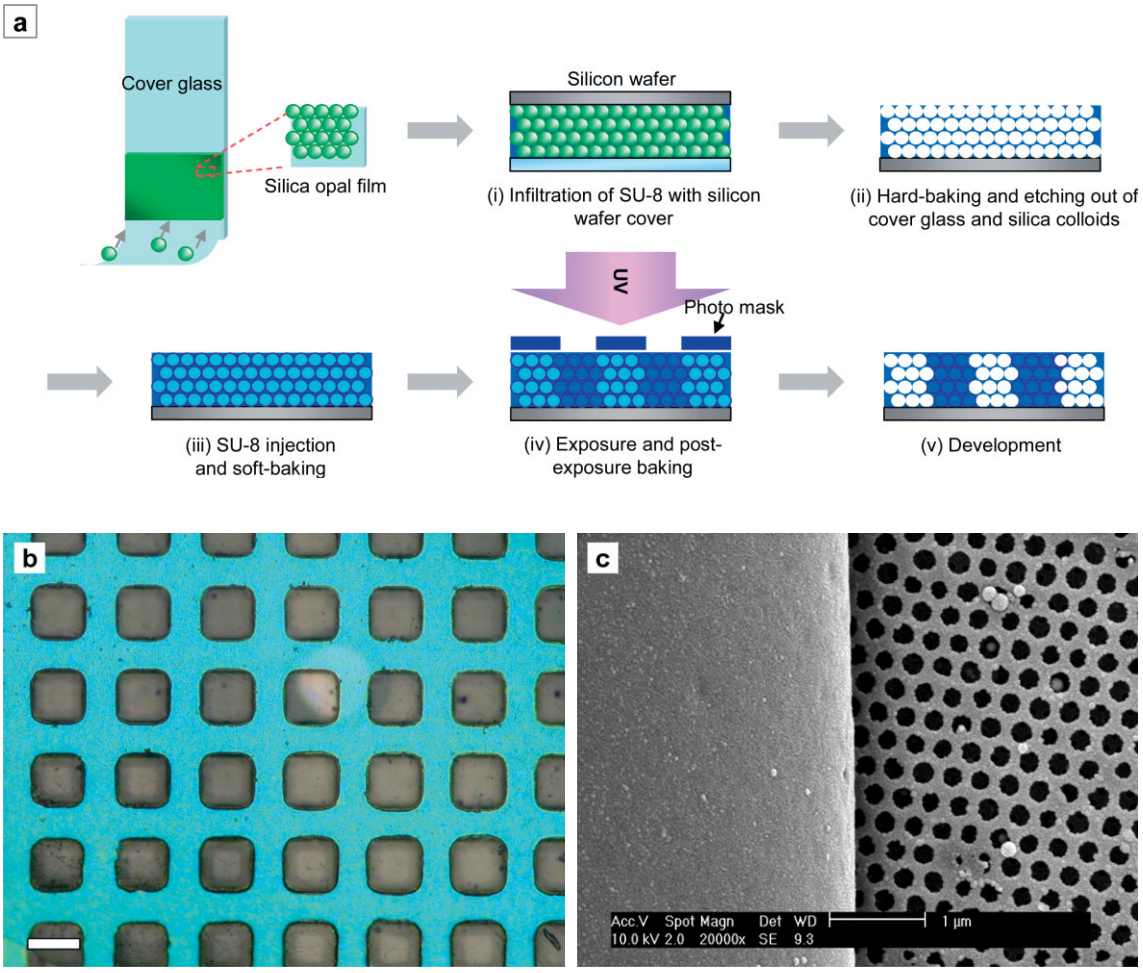

Figure 1. a) Schematic of patterned inverse opal films. First, colloidal silica films were prepared by using the dip-coating method. In step i, the SU-8 prepolymer was injected within the interstices between the colloidal silica spheres. Both cover glass and silica spheres were etched out in an HF solution, leaving hard-baked ordered macropores of SU-8 on the silicon wafer. After filling the macropores in the photoresist inverse opals with the same prepolymer, the composite films were soft-baked and then patterned using conventional photolithography. Finally, the unexposed photoresist was washed out by the developing procedure. b) Optical images of dot-patterned macroporous films. In the blue colored areas, macropores were packed in fcc lattices. (Scale bars are 50 μm.) c) Scanning electron microscopy (SEM) image that shows macroporous structures near the pattern interface.

irradiated onto the prepared composite film through a mask film with designed patterns (step iv). At the exposed spots, the soft-baked photoresist was completely crosslinked by cation-polymerization during the post-exposure baking and these spots remained transparent after development. Since the soft-baked photoresist was still soluble in the developing solution, the unexposed parts returned to their original state as an inverse opal scaffold after the developing process (step v). The prepared inverse opal film exhibited patterned reflection colors.

An optical image of an inverse opal film with a dotted pattern is shown in Figure 1b. The inverse opals of ordered macropores reflect the light selectively at a specific wavelength range depending on the pore size. In this case, we used silica spheres of 245 nm in diameter and the inverted pore size was 228 nm. Therefore, the reflected color was blue as predicted from the Bragg equation. Obviously, the exposed parts, which were filled with the hard-baked photoresist, were transparent because the refractive indices were completely matched in these regions. In this case, the exposure time was 10 s to ensure a complete curing. In Figure 1c, a scanning electron microscopy (SEM) image of a patterned inverse opal film shows the clear boundary between exposed and unexposed (porous) regions. In the unexposed porous region, macropores of an fcc symmetry with the [111] plane facing outwards were interconnected through windows.

We also developed a novel method for multicolor patterning by noting that the degree of crosslinking in the negative photoresist could be controlled by the irradiation energy of the UV light, which was adjusted mainly by the exposure time. Insufficient irradiation energy caused an incomplete curing of the photoresist that was back-filled into the macropores in the previous step. In this case, the crosslinked photoresist remained in the macropores and the uncured photoresist was washed away by the developing solution. Therefore, when the photoresist was insufficiently irradiated, the macropores were

filled partially with the polymer after development. Then, the effective refractive index (n_{eff}) of the incompletely cured macropores has increased compared to that of air (n_{air}) due to the residual polymer inside of the macropores according to the following equation:

$$n_{eff} = \sqrt{f_s n_s^2 (1 - f_s) n_{air}^2} \quad (1)$$

in which n_s and f_s are the refractive index and volume fraction of the photoresist polymer inside a macropore, respectively.

Figure 2a shows a schematic of the growth of an interior wall inside the macropores from the residual photoresist using various exposure times ranging from 0 to 10 s. As we increased the UV exposure time, the thickness of the inner wall increased and the reflection peak shifted to longer wavelengths; a 3 s exposure resulted in green and a 6 s exposure in orange light. It is noteworthy that if the exposure time exceeds 10 s, the exposed parts become transparent due to complete curing. The optical image in Figure 2b shows inverse opal films with two-color patterns that were prepared by controlling the exposure time of the UV irradiation. The orange squares were formed by UV exposure for 6.0 s on the bluish background. The background blue color was produced by the unexposed prepolymer, which led to the complete recovery of macropores. To confirm the existence of any residual polymer inside of the macropores in the UV-exposed regions, we took SEM images of the exposed and unexposed parts. As can be seen from the SEM images in Figure 2c–e, the macropores in the exposed parts were narrower than those in the unexposed

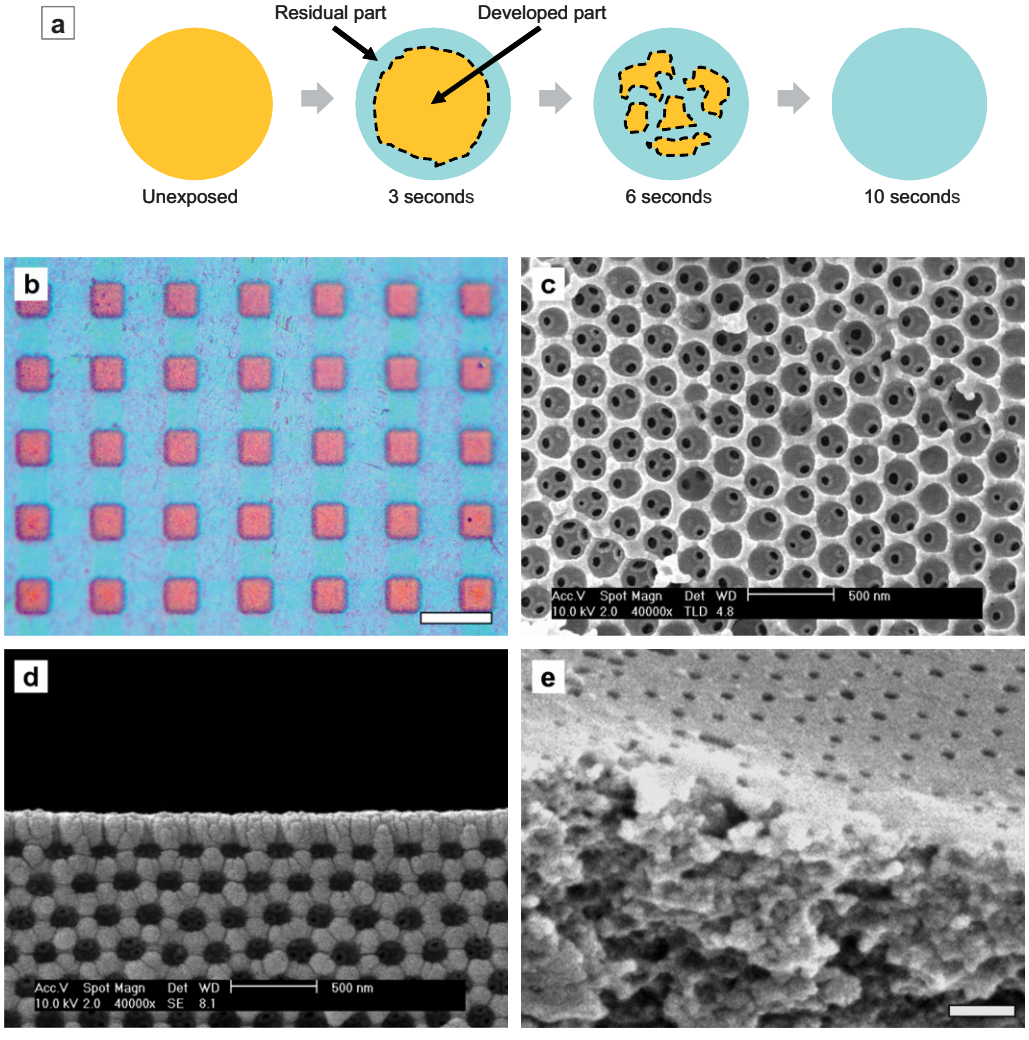

Figure 2. a) A schematic of the growth of the inner walls with an increase in the UV exposure time. As the UV exposure time was increased from 0 to 10 s, the amount of the residual photoresist inside of the macropores became larger. b) Patterned inverse opals with two different colors. Square patterns of orange and blue were generated form a dot-patterned mask. Orange dots were formed by UV exposure for 6.0 s on the blue background produced from ordered macropores. (Scale bar is 100 μm.) c–e) Cross-sectional SEM images of the film inverse opal films prepared using different UV exposure times. (Scale bars are 500 nm.) The unexposed photoresist was completely developed as shown in (c) and the residual polymers filled the macropores in the exposed regions partially, (d) and (e). The exposure times in (d) and (e) were 3.0 and 6.0 s, respectively.

ADVANCED MATERIALS

parts because of the residual polymer chains that were cross-linked partially by UV exposure. It is also obvious that the lattice constant of the inverse opals was not changed by UV exposure. Therefore, the change in the refractive-index mismatch induced by the UV exposure time shifted the reflective colors to higher wavelengths, as predicted qualitatively by Bragg's law.

Based on the precedent patterning process, novel procedures for multicolor mosaic patterns were developed as depicted in Figure 3a. In this strategy, the macropores of an SU-8 inverse opal film were first filled with the SU-8 prepolymer and exposed to UV light through a mask with stripe patterns. Then, the mask was rotated by 90° and the film was exposed again. The exposure time for each UV irradiation was shorter than 5 s, which was less than half of the exposure time required for the complete curing. Consequently, after developing and rinsing of the inverse opal film, our double exposure produced a square pattern of three different colors, as illustrated in Figure 3a. The blue squares were never exposed and the green and orange squares were exposed once and twice to UV light, respectively. The optical image of a multi-patterned inverse opal film is reproduced in Figure 3b, and the three different colors match the reflectance spectra ranging from 510 to 582 nm, as shown in Figure 3c. Superimposed spectra reflected from the patterned color pixels were obtained by using a ×10 objective lens that collected light reflected from a few pixels into the detector. The individual peaks were acquired by using a ×20 objective lens that covered only a single-color pixel. Reflectance peaks of the individual colors were broadened compared to the superimposed peaks because of a shorter focal length of the ×20 objective lens.

The shifts in the peak position induced by the selective photopolymerization matched the computational calculation of the photonic bandgap. Figure 4a and c show the simulated photonic band structures of inverse opal films that had 64 and

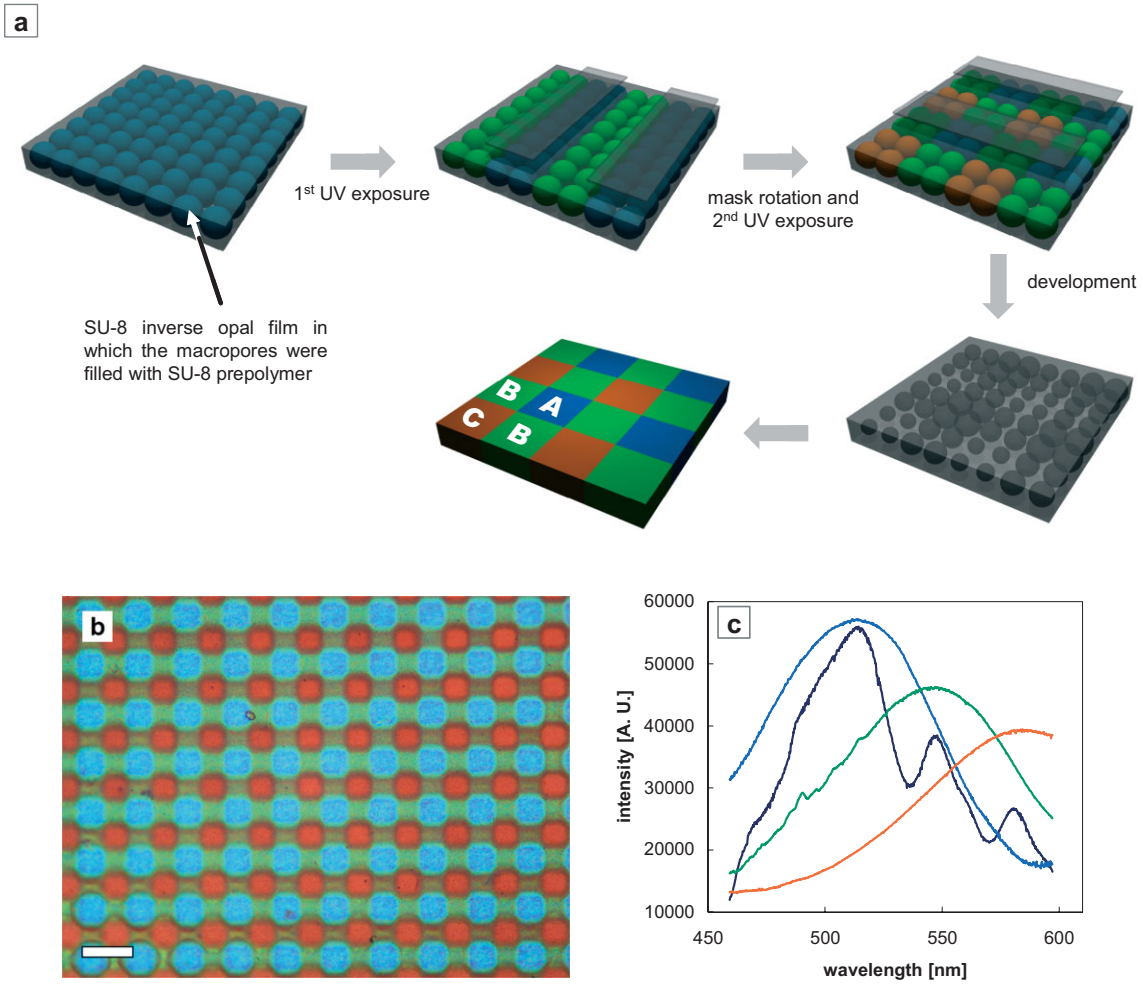

Figure 3. a) Schematic diagram for inverse opals patterned in multicolors by using double exposure. The blue color (A) indicates the area that is never exposed to UV light and the green and orange (B and C) colors indicate the areas exposed once and twice, respectively. b) Optical image of the sample created by double photolithography, in which the blue, green, and orange colors are arranged in regular patterned pixels. (Scale bar is 100 μm.) c) Reflectivity of the multicolored inverse opal patterns in (b) showing three reflection peaks which correspond to the colors observed in the optical image in (b).

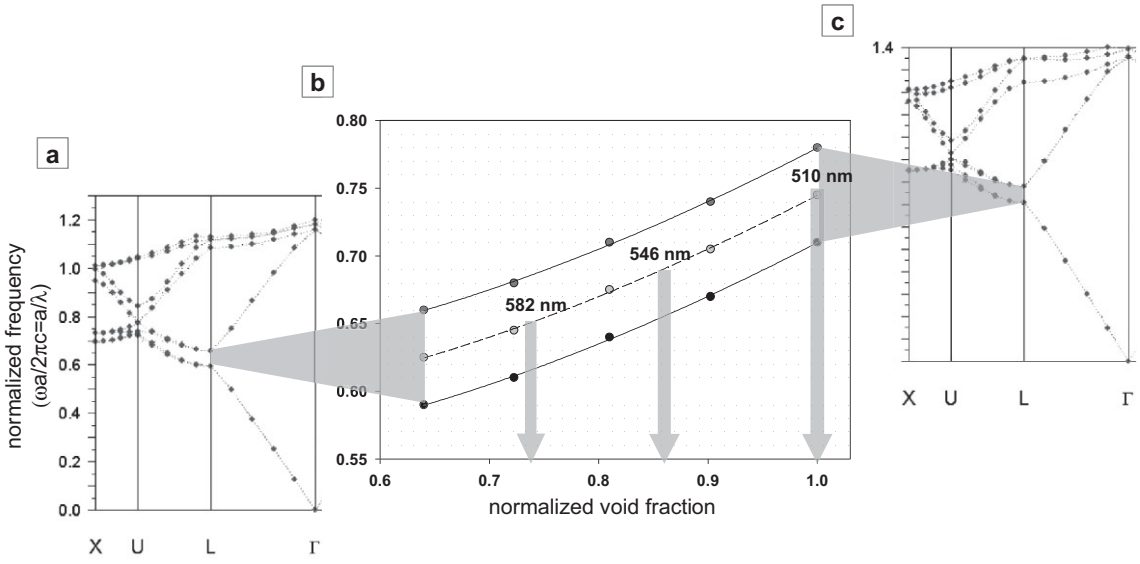

Figure 4. Photonic bandgap simulation results. a,c) Photonic bandgap diagrams of inverse opal films that have 64 and 100 % void fractions, respectively, relative to the void fraction of a close-packed inverse opal. The horizontal axis represents the wave vector in the first Brillouin zone and the vertical axis represents the normalized photonic energy. In these inverse opaline structures, the stopbands occurred between the first and second bands in the L-direction. b) Simulated bandgap of inverse opal structures as a function of the normalized volume fraction relative to the void fraction of a close-packed inverse opal. As the void fraction of the inverse opal films decreased, the L-gap was red shifted. The void fractions could also be estimated from the locations of the photonic bandgap. The three arrows represent the void fractions predicted from the corresponding experimental reflectance peaks in Figure 3c.

100 % void fractions, respectively, relative to the void fraction of a close-packed inverse opal. As the sizes of the macropores decreased from the original pore size, the L-gap shifted towards longer wavelengths. In particular, the L-gap of the original inverse opal film was located around the blue regime, which was shifted toward the red regime when the void fraction was decreased. This trend matched our experimental results which showed a red-shift during the selective photopolymerization and development. Figure 4b shows the bandgap width and location of the L-gap as a function of the relative void fraction for inverse opal films.

We demonstrated a simple and novel strategy based on conventional photolithography for patterning inverse opaline photonic crystals, which is essential for practical applications. For photonic circuit and display devices, inverse opaline photonic crystals have to be patterned into designed structures. In particular, our process is the first to materialize inverse opal structures with visible bandgaps for the fabrication of photonic devices with designed patterns. As illustrated above, pixellated photonic crystals with multicolor patterns could be fabricated by using selective photopolymerization. Pixellated photonic crystals can be used for a new type of LC microdisplay that is operated in the reflective mode. In general, reflective-mode displays make up the shortcomings of conventional transmission displays with an excellent readability under blazing sunlight. In addition, reflective-mode displays consume much less energy because they use ambient light as their light source. Therefore, reflective-mode displays are practically important for mobile electronics, such as cellular phones and personal digital assistants, because most of their power can be used as a light source for display devices. However, conventional reflective-mode displays that use color filters have serious problems in efficiency due to the doubled path length of light. When a single pixel is working, the incident light travels through the polarizer, LC cell, color filter, and reflector, and it then moves back to the front. As a result, most of the incident light is dissipated by each functional part during the path of the light.[18] Figure S2 in the Supporting Information shows schemes for three different display modes. Since the pixellated photonic-crystal films act as both the color filter and the reflector, these photonic-crystal displays have a better resolution for a given intensity of the ambient incident light than conventional reflective-mode displays.

In summary, polymeric inverse opal films were prepared by using a negative photoresist of SU-8 and silica colloidal films as sacrificial templates. Then, composite films were produced by infiltrating the same photoresist resin through the macropores of the inverse opal scaffold. Because the refractive indices of the hard-baked and the soft-baked photoresist were well matched, high-resolution patterns at the micrometer scale were obtained by using conventional photolithography. In addition, the degree of photopolymerization was controlled by adjusting the UV exposure time. The residual polymer in the macropores increased with the UV exposure time and thus the effective refractive index also increased. Consequently, the reflective color of the inverse opal could be modulated. Our photonic-crystal films have a few stop bands but do not have a complete bandgap because of an insufficient refractive-index contrast. However, the non-existence of a complete bandgap does not impose any restriction on our pixellated

ADVANCED MATERIALS

photonic crystals for microdisplays. For the microdisplays of mobile devices, the viewing angle is quite narrow and the angle dependence of the reflected colors (or stop bands) is not a major issue. Finally, since the patterning and tuning steps can be performed simultaneously in our strategy, the selective photopolymerization method can be expanded to the fabrication of 3D patterns in opaline structures.

Experimental

Synthesis of Monodisperse Colloidal Suspensions: An 8.36 wt % monodisperse silica colloidal suspension was synthesized by the Stöber method using 14 mL of tetraethylorthosilcate (TEOS 99.999 %, Sigma-Aldrich), 144 mL of ethanol (HPLC grade, Merck), 7 mL of ammonium hydroxide (26 %, Junsei), and 18 mL of ternary distilled water. The diameter of the silica spheres was 245 nm and the size distribution was less than 5 %, as measured by a dynamic light scattering system (Brookhaven Instruments Corp.).

Dip-Coating and Structure Inversion: Uniform silica colloidal crystal films were deposited on microscope cover glasses (12-545J, Fisher Scientific) by the dip-coating method. Then, the photoresist (SU-8 25, Microchem) was infiltrated into the colloidal crystal films and soft-baked at 70 °C for 12 h in a vacuum oven. The soft-baked resin was then hard-baked at 195 °C for 30 min. The silica particles were etched out using a 5 % HF solution (50 %, Sigma–Aldrich).

Patterning Inverse Opals: After washing and drying, the inverse opals were infiltrated again with the same photoresist and soft-baked. For the completely crosslinked patterns, the samples were exposed to UV light for 10 s through a 50 μm lined or dotted mask. For incomplete development, we applied UV light for less than 10 s (3 s for green and 6 s for orange light). The exposed films were then post-baked again at 95 °C for 4 min. Finally, the exposed films were developed with PGMEA (1-methoxy-2-propyl acetate, 99 %, Sigma–Aldrich) and rinsed with isopropanol (HPLC grade, Merck).

Characterization: Optical images were taken using a digital camera mounted on a Nikon L-150 microscope. SEM images were taken using a Philips XL20SFEG scanning electron microscope. The reflectance spectra of the patterned inverse opal films with three different colors were measured using a spectrophotometer with a microscope ×10 objective lens (LU Plan, Nikon) and the incident light was aligned normal to the surface. Individual peaks were obtained by using a ×20 objective lens (LU Plan, Nikon), which focused the incident light to the individual pixels.

Received: December 8, 2005
Final version: May 4, 2006
Published online: July 25, 2006

[1] T. A. Taton, D. J. Norris, *Nature* **2002**, *416*, 685.
[2] A. Imhof, D. J. Pine, *Nature* **1997**, *389*, 948.
[3] P. Jiang, J. F. Bertone, K. S. Hwang, V. L. Colvin, *Chem. Mater.* **1999**, *11*, 2132.
[4] K.-H. Lin, J. C. Crocker, V. Prasad, A. Schofield, D. A. Weitz, T. C. Lubensky, A. G. Yodh, *Phys. Rev. Lett.* **2000**, *85*, 1770.
[5] T. Ruhl, P. Spahn, H. Winkler, G. P. Hellmann, *Macromol. Chem. Phys.* **2004**, *205*, 1385.
[6] V. Kitaev, G. A. Ozin, *Adv. Mater.* **2003**, *15*, 75.
[7] Q.-B. Meng, C.-H. Fu, Y. Einaga, Z.-Z. Gu, A. Fujishima, O. Sato, *Chem. Mater.* **2002**, *14*, 83.
[8] S. M. Yang, H. Miguez, G. A. Ozin, *Adv. Funct. Mater.* **2002**, *12*, 425.
[9] P. Yang, T. Deng, D. Zhao, P. Feng, D. Pine, B. F. Chmelka, G. M. Whitesides, G. D. Stucky, *Science* **1998**, *282*, 2244.
[10] P. Jiang, G. N. Ostojic, R. Narat, D. M. Mittleman, V. L. Colvin, *Adv. Mater.* **2001**, *13*, 389.
[11] P. Yang, A. H. Rizvi, B. Messer, B. F. Chmelka, G. M. Whitesides, G. D. Stucky, *Adv. Mater.* **2001**, *13*, 427.
[12] W. Lee, S. A. Pruzinsky, P. V. Braun, *Adv. Mater.* **2002**, *14*, 271.
[13] Z.-Z. Gu, A. Fujishima, O. Sato, *Angew. Chem. Int. Ed.* **2002**, *41*, 2067.
[14] K. Yoshino, S. Satoh, Y. Shimoda, H. Kajii, T. Tamura, Y. Kawagishi, T. Matsui, R. Hidayat, A. Fujii, M. Ozaki, *Synth. Met.* **2001**, *121*, 1459.
[15] D. Kang, J. E. Maclennan, N. A. Clark, A. A. Zakhidov, R. H. Boughman, *Phys. Rev. Lett.* **2001**, *86*, 4052.
[16] P. Jiang, K. S. Hwang, D. M. Mittleman, J. F. Bertone, V. L. Colvin, *J. Am. Chem. Soc.* **1999**, *121*, 11 630.
[17] J. H. Moon, A. Small, G.-R. Yi, S.-K. Lee, W.-S. Chang, D. J. Pine, S.-M. Yang, *Synth. Met.* **2005**, *148*, 99.
[18] S.-T. Wu, D.-K. Yang, *Reflective Liquid Crystal Displays*, John Wiley & Sons Ltd, Chichester, UK **2001**.

